Title

Temperature and Humidity Stable Alkali/Alkaline-Earth Metal Carbonates as Electron Heterocontacts for Silicon Photovoltaics

Journal

Advanced Energy Materials, 8(22)

ISSN

1614-6832

Authors

Wan, Yimao
Bullock, James
Hettick, Mark
et al.

Publication Date

2018-08-01

DOI

10.1002/aenm.201800743

Peer reviewed

Article type: Communication

Thermally and Environmentally Stable Alkali/Alkaline-Earth Metal Carbonates as Electron Heterocontacts for Silicon Photovoltaics

Yimao Wan, James Bullock, Mark Hettick, Zhaoran Xu, Chris Samundsett, Di Yan, Jun Peng, Ali Javey, and Andres Cuevas*

Dr. Yimao Wan, Chris Samundsett, Dr. Di Yan, Jun Peng, and Prof. Andres Cuevas

[1] Research School of Engineering, The Australian National University (ANU), Canberra, ACT 0200, Australia

(Email: yimao.wan@anu.edu.au)

Dr. Yimao Wan, Dr. James Bullock, Mark Hettick, Zhaoran Xu, Prof. Ali Javey

[2] Department of Electrical Engineering and Computer Sciences, University of California, Berkeley, California 94720, USA

[3] Materials Sciences Division, Lawrence Berkeley National Laboratory, Berkeley, California 94720, USA

Keywords: alkali carbonate, alkaline earth metal carbonates, electron heterocontact, silicon photovoltaics

Abstract

Nanometre scale interfacial layers between the metal cathode and the *n*-type semiconductor play a critical role in enhancing the transport of charge carriers in and out of optoelectronic devices. Here, a range of nanoscale alkali and alkaline earth metal carbonates (i.e., potassium, rubidium, caesium, calcium, strontium, and barium) are shown to function effectively as electron heterocontacts to lightly doped *n*-type crystalline silicon (c-Si), which is particularly challenging to contact by common metals. These carbonate inter-layers are shown to significantly enhance the performance of *n*-type c-Si proof-of-concept solar cells up to a power conversion efficiency of ~19%. Furthermore, these devices are thermally stable up to 350 °C and both the caesium and barium carbonates pass a standard 1000-hour damp heat test, with > 95% of their initial performance maintained. Electron heterocontacts based on alkali and alkaline earth metal carbonates show a high potential for industrial feasibility and longevity for deployment in the field.

A key metric of a metal to silicon contact is the barrier height (Φ_B), predicted by the Schottky-Mott rule to be the difference between the metal work function and silicon's electron affinity.[1,2] Usually, the observed Φ_B differs significantly from the calculated one, due to the Fermi-level pinning phenomenon, consequence of a high density of states within the energy bandgap at the metal/silicon interface. Besides the conventional approach of heavily doping the silicon surface in order to make the Schottky barrier thin enough for carrier tunnelling, an alternative approach is to employ a thin interfacial layer between metal and silicon to reduce the defect density at the interface, thus releasing the Fermi level. This means, on the one hand, that the work function of the contacting materials needs to be carefully selected for either *n*-type or *p*-type silicon; on the other hand, the defect-passivating interlayer can hinder the transport of carriers. For a low-resistance Ohmic contact to *n*-type silicon (*n*-Si), it is desirable that the interfacial layer also has the function of reducing the work function of the outer metal in order to facilitate electron ejection (in the case of solar cells) or injection (for other devices). Recently, several dopant-free interfacial materials have been shown to provide a low resistivity Ohmic contact to *n*-Si, including lithium fluoride,[3-5] magnesium fluoride,[6] magnesium oxide,[7] titanium oxide,[8,9] tantalum oxide,[10] and their combinations.[11]

Another class of candidate materials are the alkali and alkaline-earth metal carbonates which until now have mostly been explored in organic electronics due to their ability to facilitate electron injection. The application of these carbonates to silicon solar cells is only incipient, and it

has been limited to caesium carbonate.[12,13] In this work, we present a comprehensive experimental study of a range of carbonates ($K_2C_xO_y$, $Rb_2C_xO_y$, $Cs_2C_xO_y$, CaC_xO_y, SrC_xO_y, and BaC_xO_y) as electron contacts for silicon solar cells. We first investigate the electronic band structure and conduction properties of the thermally evaporated carbonates, capped with aluminium as the metallic electrode. After optimising these electron contacts in terms of contact resistivity, they are applied to the full rear surface of *n*-type silicon solar cells, achieving a fill factor of ~80% and a power conversion efficiency of ~19%. Thermal and environmental stability tests are then performed, showing that these devices are stable up to 350 °C and that both the caesium and barium carbonates pass an accelerated environmental test at 85 °C and 85% humidity for 1000 hours.

The electronic band structure was characterized via X-ray photoelectron spectroscopy (XPS), including core level and valence band. Figure 1(a) shows the core levels of C 1s spectra for four of the carbonates, except for the case of potassium and calcium because of their extremely poor stability in air and even in a nitrogen glove box, owing to the loose packing of relatively large carbonate anions and small metal ions.[14] The C 1s spectrum is decomposed into three parts: main carbonate at ~289.5 eV, hydrocarbonate at ~288 eV, and adventitious carbon at ~285 eV.[15] All four materials exhibit significant adventitious carbon probably due to organic contaminants during evaporation, transportation and/or measurement. The hydrocarbonate signal is anticipated to originate from the interaction with moisture. The signal is more pronounced for alkali carbonates than alkaline earth ones. This is within expectations, since

alkali carbonates are much more hygroscopic. Particularly for Ba carbonate, the signal for hydrocarbonate is negligible, indicating that the material is more stable against moisture or air ambient, which is confirmed by the environmental tests at the device level presented below. It is worth noting that the pronounced carbon component observed in this work contradicts previous reports for Cs_2CO_3, which mention its decomposition into caesium oxide, with negligible release of carbon. The discrepancy might originate from a different degree of decomposition of Cs_2CO_3 during thermal evaporation. The stoichiometry of the four films measured by XPS is summarised in Table I. It shows that the composition of the alkali carbonates is richer in C and O than the alkaline earth metal ones, presumably due to their higher hygroscopicity. It is also noticeable that the stoichiometry of the alkaline earth metal carbonates is slightly metal rich.

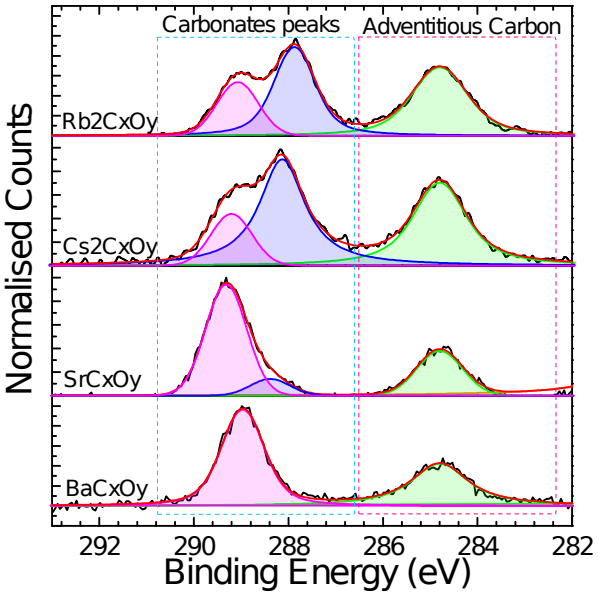

Figure 1: The core level spectrum of C1s of thermally evaporated carbonate films measured by X-ray photoelectron spectroscopy (XPS) measurements. The extracted stoichiometry is summarised in Table I. The spectra is for the four of

the carbonates, except for the case of potassium and calcium because of their exceptionally extremely poor stability in air and even in a nitrogen glove box.

Table I. Summary of stoichiometry and work function of thermally evaporated carbonates

Material	**Stoichiometry**		**Work function (eV)**
	x	y	
$Rb_2C_xO_y$	1.23	4.48	2.66
$Cs_2C_xO_y$	0.87	3.09	2.36
SrC_xO_y	0.55	2.92	2.81
BaC_xO_y	0.59	2.51	2.23

The work function of the four carbonates is determined by the XPS secondary electron cut-off. The results, shown in Figure 2(a) and summarised in Table I indicate that all four carbonates exhibit an extremely low work function, ranging from 2.23 to 2.81 eV, in good agreement with the value for Cs_2CO_3 (~2.2 eV) reported Huang et al.[16] Given that the XPS measurements were performed for carbonate films capped with Al, these results demonstrate their ability to strongly reduce the work function of the contact, which for pure Al is ~4.1 eV.[2] One of the tentative hypothesis for the origin of such a low work function is the reaction of Al metal with the carbonate, resulting in the formation of Al–O–M (where M represents the Alkali or Alkaline metal).[16] The reduced work function is anticipated to promote downward band-bending inside the silicon wafer, drawing electrons to the surface and consequently improving electron transport, as illustrated schematically in Figure 2(b).

The electrical contact behaviour of the carbonate/Al electrodes onto *n*-Si is evaluated by measuring the contact resistivity ρ_c using the method devised by Cox and Strack,[17] as shown schematically in the inset of Figure 2(c). A series of representative *I*–*V* measurements of samples without and with 1 nm of six different carbonate interlayers between Al and *n*-Si is shown in Figure 2(c). As we can see in this figure, the sample with Al directly on *n*-Si (i.e., without a carbonate interlayer) exhibits a high contact resistivity ρ_c of ~5 Ωcm^2 and a non-linear behaviour for negative bias. In contrast, the insertion of a nanoscale carbonate (~1 nm) film enhances the contact very substantially, with a perfectly Ohmic behaviour (i.e., a linear *I*–*V* curve). The extracted ρ_c for the six carbonates is plotted as a function of film thickness in Figure 2(d). It can be seen that, for all the six carbonates explored in this work, the insertion of a 0.5 nm carbonate interlayer induces a dramatic decrease of ρ_c by more than one order of magnitude. The ρ_c reaches a minimum for a film thickness of ~1 nm, and then it increases rapidly for film thickness above 5 nm. This dependence of ρ_c on film thickness is similar to that observed for fluorides and oxides. The likely reasons for the low resistance for electron transport provided by the carbonate/Al contacts could be (*i*) their low work function, which creates an accumulation of electrons at the interface, and/or (*ii*) the release of the Fermi-level via the passivation of defects at the silicon surface. The solar cell device results presented below indicate that the level of passivation is relatively modest and, therefore, the low work function is most likely the main reason for the low contact resistance.

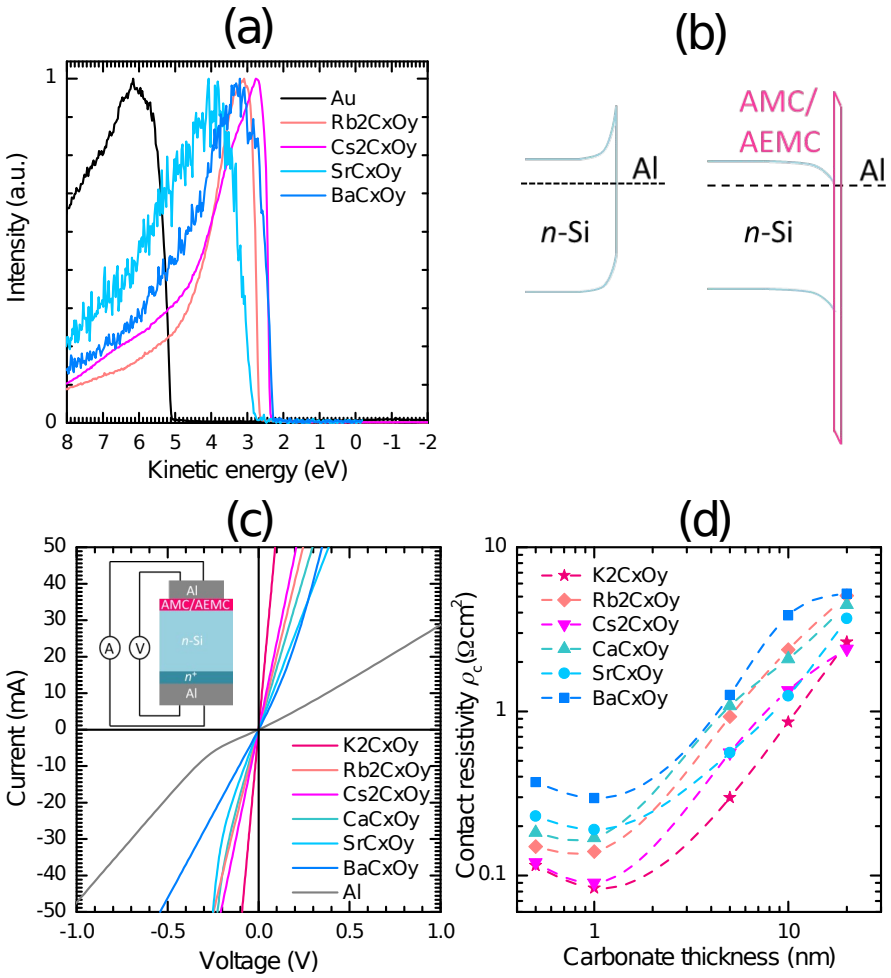

Figure 2: (a) shows the secondary electron cut-off spectrum measured at the carbonates/Al interface with a gold (Au) reference. (b) depicts the schematic of energy band diagram with and without carbonate interfacial layers. (c) presents a series of *I*–*V* measurements of samples with 1 nm carbonate interlayer between Al and *n*-type c-Si. Schematic of the contact resistivity test structure is included in inset. (d) shows the contact resistivity ρ_c as a function of carbonate thickness.

The six different carbonate (~1 nm) /Al (~200 nm) electron contacts were integrated in the complete *n*-type silicon solar cells as a full area rear contacts, as schematically depicted in Figure 3(a). The *J*–*V* photovoltaic characteristic curves under one sun standard illumination are plotted in Figure 3(b) for cells with and without carbonate interlayers (i.e., the

control cell with Al directly on *n*-Si). The detailed electrical parameters of all the cells are given in Figure 3(c). As expected from the contact resistance measurements, the insertion of a 1 nm thick interfacial layer enhances substantially all cell parameters for all six carbonates. The highest power conversion efficiency of 19.4% in this set of experiments is obtained for potassium carbonate, with open-circuit voltage (V_{OC}), short-circuit current (J_{SC}) and fill factor (*FF*) of 624.3 mV, 38.89 mA/cm^2 and 79.94%, respectively. Compared to the control cell (i.e., without a carbonate interlayer), an absolute 30 to 60 mV increase of V_{OC} is observed. Although this may be taken as proof of some level of passivation of the silicon surface by the carbonates, it is important to keep in mind that the contact between Al and *n*-Si in the control cell is not perfectly Ohmic and can originate a small loss of voltage in the device. The fact that the short-circuit current is also higher for the devices with a carbonate/Al contact tends to support the hypothesis of a mild surface passivating effect. Nevertheless, V_{OC} is more sensitive to surface passivation, and the values measured for these cells are not consistent with high quality passivation. Further work should explore the addition of extra interlayers to improve the passivation quality. Another significant gain in cell performance comes from an increase of *FF* by an absolute 5.5%, which is directly attributable to the reduction of the contact resistivity presented in Figure 2. Globally, the improvement in V_{OC}, J_{SC} and *FF* demonstrates very promising electron selective properties for these alkali and alkaline earth metal carbonates.

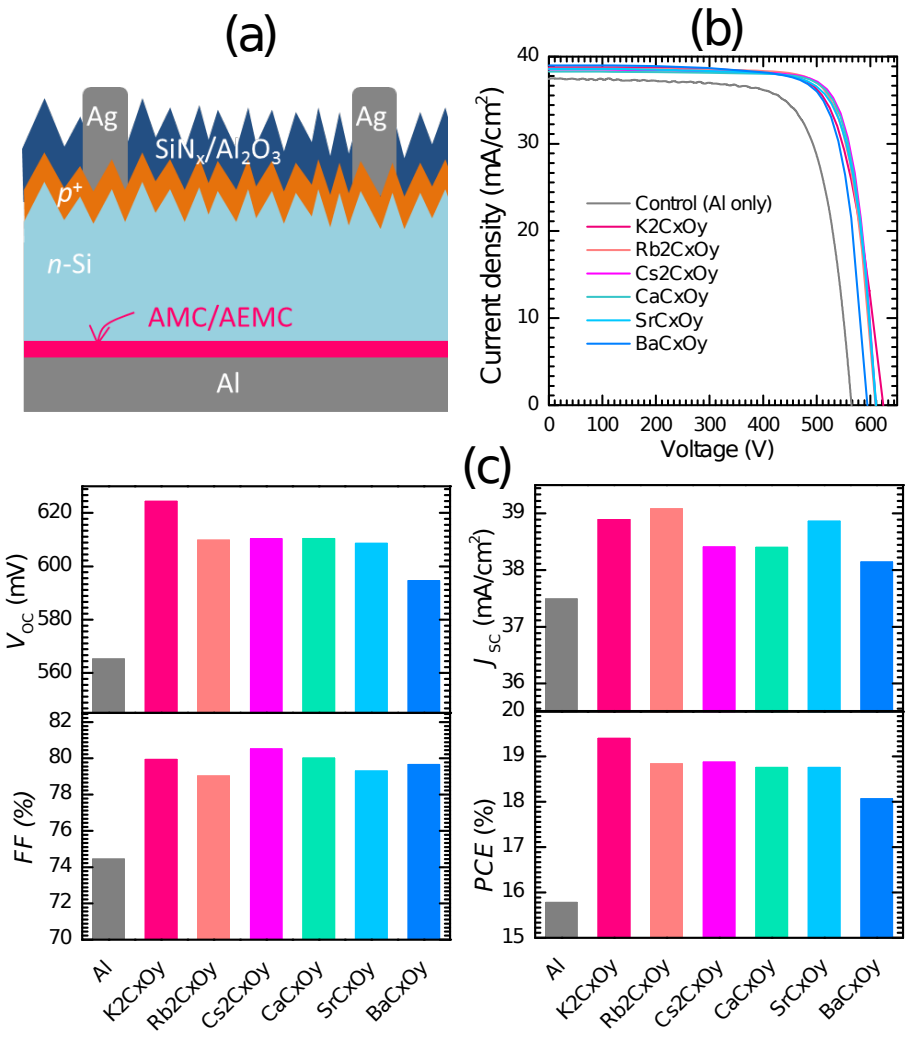

Figure 3: Device results with full-area rear carbonate electron heterocontacts. (a) shows the silicon solar device schematic. (b) presents the light *J–V* behavior measured under standard one sun conditions for cells without and with ~1 nm carbonate interlayers. (c) shows the detailed electrical parameters (V_{OC}, J_{SC}, *FF and PCE*) for different carbonate films.

For any new contact-formation technology, even if successful in the lab, the thermal stability and environment reliability of the solar cell devices remain as important considerations. One set of solar cells with ~1 nm carbonate interlayers was annealed in forming gas for 10 minutes at

different temperatures in the range 250 ºC – 500 ºC, whereas another set was submitted to a standard 1000-hour damp heat test at 85 ºC and 85% relative humidity. The relative change of the electrical parameters of the solar cells with respect to the control devices before treatment is plotted in Figures 4 (a) and (b) for the two tests, respectively. As can be seen in Figure 4(a), the cell parameters are essentially stable up to 350 °C for all the carbonates, and then start deteriorating when the annealing temperature increases further. It is worth mentioning that we do not observe a significant difference in thermal stability among the six carbonates studied here. In contrast, only the solar cells with $Cs_2C_xO_y$ and BaC_xO_y contacts survive the 1000-hour damp heat test, maintaining > 95% of their initial performance. This behaviour might be related to the fact that the two metal ions have the largest atomic numbers of the six explored here.[18]

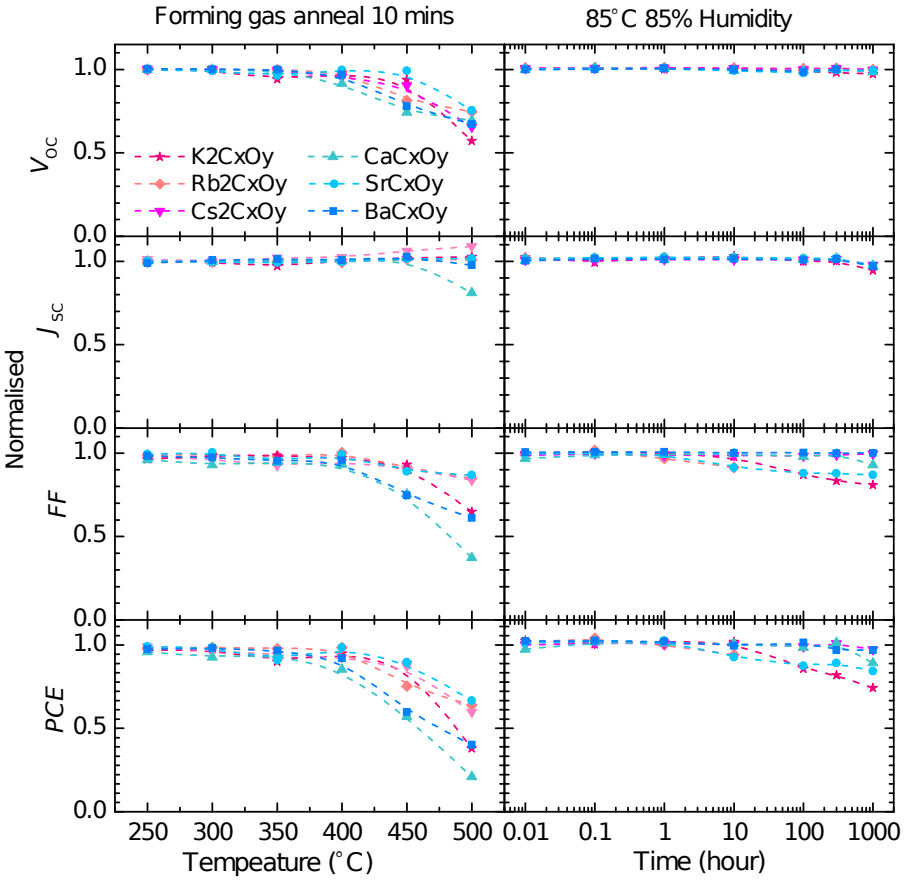

Figure 4: Thermal and environmental stability of the solar devices. The relative changes in electrical parameters (V_{OC}, J_{SC}, *FF*, and *PCE*) are plotted as function of annealing temperature and damp heat test duration.

In summary, six different alkali and alkaline earth metal carbonates have been demonstrated to function as effective and stable electron contacts for silicon solar cells, enabling significant gains in performance over a control device with Al directly on *n*-Si. It is further shown that all the carbonate/Al contacted solar cells are thermally stable up to 350 °C, and that two of the carbonate/Al contacts (Cs and Ba) pass the standard 1000-hour damp heat test at 85°C and 85% relative humidity. The abundance, low temperature deposition, and simple, yet effective, electron contact structure of these materials, pave the way for designing and fabricating novel cathodes for low-cost silicon solar cells.

Experimental Section

Carbonates films were thermally evaporated at a rate of 0.1 Å/s and a base pressure of $< 1 \times 10^{-6}$ Torr from a series of Sigma-Aldrich carbonate powder sources, as summarised below.

Material	Potassium carbonate	Rubidium carbonate	Caesium carbonate	Calcium carbonate	Strontium carbonate	Barium carbonate
Purity (%)	99.995	99.8	99.995	99.999	99.995	99.999

XPS characterizations were performed on carbonates/Al coated single-side polished c-Si wafers using a Kratos AXIS Ultra DLD system, under ultrahigh vacuum with a monochromatic Al Kα X-ray source and a hemispherical analyzer. Secondary electron cut-off with X-ray excitation was employed for work function measurements. Voigt lineshapes were used to fit core level spectra, and film stoichiometry was extracted based on the resulting peak areas. A gold reference was used in the same session to verify instrument work function, and to provide a reference for the work functions reported.

Contact resistivity test samples for carbonates/Al electron contacts were fabricated on Czochralski (Cz) *n*-Si wafers. Shadow masks were used to pattern an array of circular pads with different diameters upon thermal evaporation. The rear of the contact samples was phosphorus diffused (n^+) to minimize the contribution of the rear Al/Si contact. A Keithley 2425 source–meter was used to conduct current–voltage (*I*–*V*) measurements at room temperature. The resistance versus diameter trend was fitted with a spreading resistance model, enabling extraction of contact resistance ρ_c.

Proof-of-concept solar cells were fabricated on Cz *n*-Si wafers with a resistivity of ~1.0 Ωcm and a thickness of ~180 μm. The sunward side of cells features an array of random pyramids,[19-23] ~110 Ω/□ boron diffusion, and then ~20 nm ALD Al_2O_3 and ~65 nm PECVD silicon nitride.[24] The rear silicon surfaces were then coated with the carbonates electron contacts (i.e., ~1 nm carbonates / 200 nm Al). The front metal grid contacts with 10 μm width lines and 1.3 mm pitch were patterned via photolithography, followed by thermal evaporation of a Cr (~10 nm) / Pd (~10 nm) / Ag (~100 nm) stack, and finally thickened by Ag electroplating. The light *J*–*V* behaviour was measured by a solar simulator from Sinton Instruments under standard one sun conditions (100 mW/cm^2, AM1.5 spectrum, 25 °C), calibrated with a certified Fraunhofer CalLab reference cell.

Acknowledgements

This work was supported by the Australian Government through the Australian Research Council (Discovery Project: DP150104331) and the Australia−US Institute for Advanced

Photovoltaics (AUSIAPV) program under Grant Number ACAP6.9. Y.W. is holding Individual Fellowship from Australian Center of Advanced Photovoltaics (ACAP). The XPS characterization was performed at the Joint Center for Artificial Photosynthesis, supported through the Office of Science of the US Department of Energy under Award Number DE-SC0004993. A.J., M.H. and J.B. acknowledge funding from the Bay Area Photovoltaics Consortium (BAPVC).

References

[1] Dieter K. Schroder, *Semiconductor material and device characterization*, 3rd ed. (John Wiley & Sons Inc., Hoboken, New Jersey, USA, **2006**).
[2] S. M. Sze and K. K. Ng, *Physics of Semiconductor Devices*. (John Wiley & Sons, **2006**).
[3] Yunfang Zhang, Ruiyuan Liu, Shuit-Tong Lee, and Baoquan Sun, Applied Physics Letters 104 (8), 083514 (**2014**).
[4] J. Bullock, M. Hettick, J. Geissbühler, A. J. Ong, T. Allen, C. M. Sutter-Fella, T. Chen, H. Ota, E. W. Schaler, S. De Wolf, C. Ballif, A. Cuevas, and A. Javey, Nature Energy 1 (15031) (**2016**).
[5] James Bullock, Peiting Zheng, Quentin Jeangros, Mahmut Tosun, Mark Hettick, Carolin M Sutter-Fella, Yimao Wan, Thomas Allen, Di Yan, and Daniel Macdonald, Advanced Energy Materials (**2016**).
[6] Yimao Wan, Christian Samundsett, James Bullock, Thomas Allen, Mark Hettick, Di Yan, Peiting Zheng, Xinyu Zhang, Jie Cui, and Josephine Anne McKeon, ACS applied materials & interfaces (**2016**).
[7] Yimao Wan, Chris Samundsett, James Bullock, Mark Hettick, Thomas Allen, Di Yan, Jun Peng, Yiliang Wu, Jie Cui, Ali Javey, and Andres Cuevas, Advanced Energy Materials 7 (5), 1601863 (**2017**).
[8] Sushobhan Avasthi, William E. McClain, Gabriel Man, Antoine Kahn, Jeffrey Schwartz, and James C. Sturm, Applied Physics Letters 102 (20) (**2013**).
[9] Xinbo Yang, Peiting Zheng, Qunyu Bi, and Klaus Weber, Solar Energy Materials and Solar Cells 150, 32 (**2016**).
[10] Yimao Wan, Siva Krishna Karuturi, Christian Samundsett, James Bullock, Mark Hettick, Di Yan, Jun Peng, Parvathala Reddy Narangari, Sudha Mokkapati, Hark Hoe Tan, Chennupati Jagadish, Ali Javey, and Andres Cuevas, ACS Energy Letters 3 (1), 125 (**2018**).
[11] James Bullock, Yimao Wan, Zhaoran Xu, Stephanie Essig, Mark Hettick, Hanchen Wang, Wenbo Ji, Mathieu Boccard, Andres Cuevas, Christophe Ballif, and Ali Javey, ACS Energy Letters, 508 (**2018**).
[12] Yunfang Zhang, Wei Cui, Yawen Zhu, Fengshuo Zu, Liangsheng Liao, Shuit-Tong Lee, and Baoquan Sun, Energy & Environmental Science 8 (1), 297 (**2015**).
[13] James Bullock, Yimao Wan, Mark Hettick, Jonas Geissbühler, Alison J. Ong, Daisuke Kiriya, Di Yan, Thomas Allen, Jun Peng, Zhang Xinyu, Carolin M. Sutter-Fella, Stefaan De Wolf, Christophe Ballif, Andrés Cuevas, and Ali Javey, presented at the IEEE 43rd Photovoltaic Specialist Conference (PVSC), Portland, Oregon, **2016**.
[14] F.A. Cotton and G. Wilkinson, *Advanced Inorganic Chemistry*. (John Wiley &; Sons, **1988**).
[15] A. V. Shchukarev and D. V. Korolkov, Central European Journal of Chemistry 2 (2), 347 (**2004**).
[16] J. Huang, Z. Xu, and Y. Yang, Advanced Functional Materials 17 (12), 1966 (**2007**).
[17] R. H. Cox and H. Strack, Solid-State Electronics 10 (12), 1213 (**1967**).
[18] Ki Chang Kwon, Kyoung Soon Choi, Buem Joon Kim, Jong-Lam Lee, and Soo Young Kim, The Journal of Physical Chemistry C 116 (50), 26586 (**2012**).

[19] M. G. Coleman W. L. Bailey, C. B. Harris, and I. A. Lesk, U.S. Patent No. 4137123 (**Jan. 30, 1979**).
[20] Osamu Tabata, Ryouji Asahi, Hirofumi Funabashi, Keiichi Shimaoka, and Susumu Sugiyama, Sensors and Actuators A: Physical 34 (1), 51 (**1992**).
[21] L. M. Landsberger, S. Naseh, M. Kahrizi, and M. Paranjape, Microelectromechanical Systems, Journal of 5 (2), 106 (**1996**).
[22] Jae Sung You, Donghwan Kim, Joo Youl Huh, Ho Joon Park, James Jungho Pak, and Choon Sik Kang, Solar Energy Materials and Solar Cells 66 (1–4), 37 (**2001**).
[23] P. Papet, O. Nichiporuk, A. Kaminski, Y. Rozier, J. Kraiem, J. F. Lelievre, A. Chaumartin, A. Fave, and M. Lemiti, Solar Energy Materials and Solar Cells 90 (15), 2319 (**2006**).
[24] Yimao Wan, Keith R McIntosh, Andrew F Thomson, and Andres Cuevas, IEEE Journal of Photovoltaics 3 (1), 554 (**2013**).